



X 1.11

Conference
Preprint 118

SATURN HISTORY DOCUMENT
University of Alabama Research Institute
History of Science & Technology Group

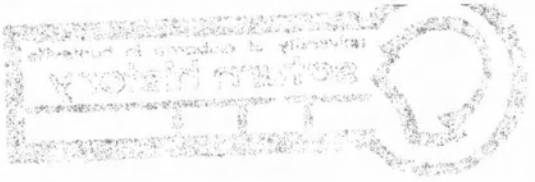
Date ----- Doc. No. -----

Structural Problems of Large Space Boosters

Emil A. Hellebrand



Presented at the ASCE Structural Engineering
Conference and Annual Meeting October 19-23, 1964



The symbols on the cover are graphic representation of the Technical Divisions participating in the Structural Engineering Conference and Annual Meeting/October 19-23, 1964. Reading from top to bottom, the Divisions are: Soil Mechanics and Foundations, Construction, Structural, Waterways and Harbors, Hydraulics, and Engineering Mechanics.

This preprint has been provided for the convenience of distributing information immediately after presentation. No acceptance or endorsement of the American Society of Civil Engineers is implied; the Society is not responsible for any statement made or opinion expressed in its publications. To defray, in part, the cost of preprinting, a charge of 50 cents per copy has been established.

STRUCTURAL PROBLEMS OF LARGE SPACE BOOSTERS

by Emil A. Hellebrand

Introduction:

The sheer size of today's space vehicles and the cost sensitivity of \$/lb. payload in orbit necessitate careful analysis and testing of structures to a degree unheard of a few years ago. Our biggest problems lie in the area of structural dynamics, control feedback and coupling of propulsion, that is pump induced flow pulsation, with engine thrust output and structural modes.

I would like to give you two examples of past and current studies we make at Marshall Space Flight Center to insure that space vehicles of the Saturn family are structurally sound, stable and efficient.

Let me first talk about

Space Vehicle Configuration Optimization

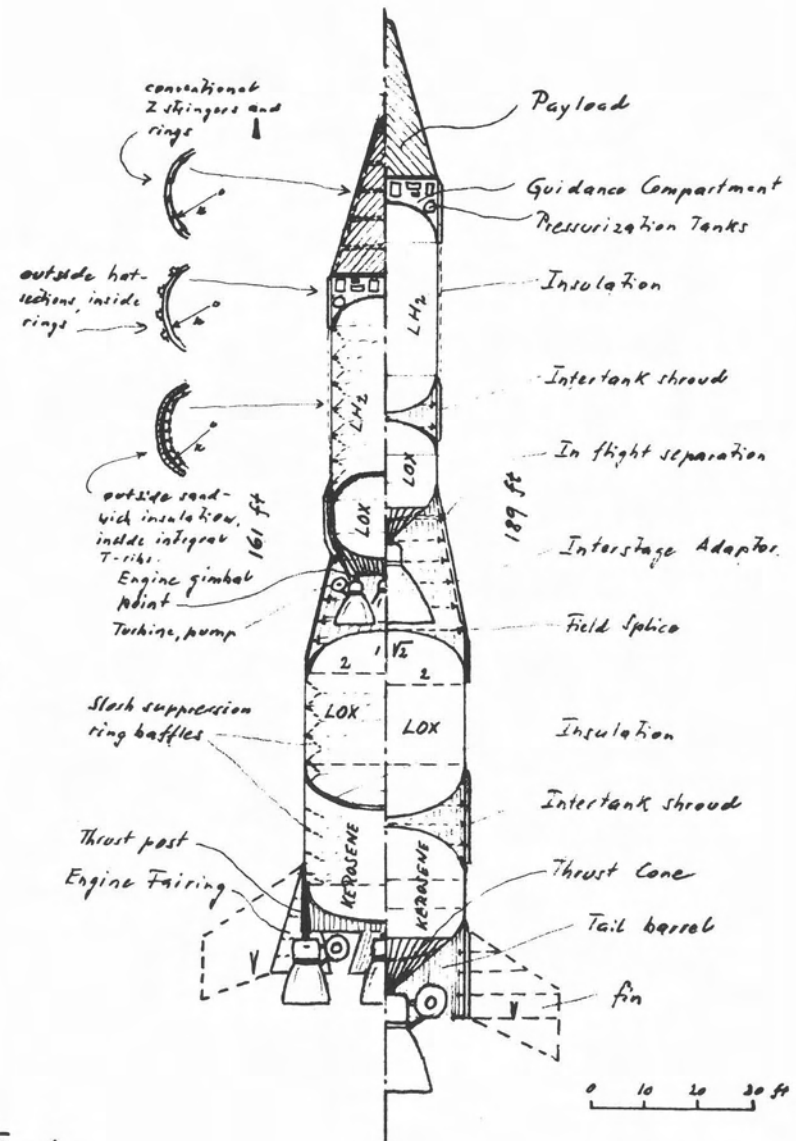
Configuration optimization improves vehicle design efficiency in two ways, (a) by making maximum use of internal pressure to reduce compressive forces that lead to structural instability and (b) by reducing overall vehicle length to increase bending, torsional and longitudinal frequencies to minimize control feedback and coupling of longitudinal structural modes with liquid column modes and pump induced thrust oscillations, the "POGO" effect. Increased lateral and longitudinal frequencies also reduce dynamic overshoots due to gust forces, rapid thrust buildup, and rebound at engine shutoff, especially under launching pad abort conditions.

Mr. Hellebrand is currently Deputy Director, Propulsion and Vehicle Engineering Laboratory, George C. Marshall Space Flight Center, National Aeronautics and Space Administration

Structural instability is sensitive to a great many influences such as slight deviations in geometry, residual stresses and local discontinuities and a standard deviation of as much as 15 percent of the strength mean is not uncommon. Internal pressure, however, increases the buckling strength by improving geometry and reduces dispersions considerably.

Vehicle length to maximum diameter ratios of from 8 to 10 lead to minimum weight designs. If this ratio drops below 8, bulkheads and thrust distribution structures become too large and too heavy and their spring rates become low enough to induce local dynamic effects on structures and liquids that again interfere with the functions of propulsion and vehicle control. On the other hand, a ratio above 10 increases lateral dynamic beam effects, reduces lateral frequencies and increases control feedback.

Figure No. 1 shows a two-stage Saturn class vehicle with typical tank and engine configurations and some basic design details. The right half shows separate propellant tanks and one center engine. This arrangement will not yield minimum structural weights because large portions of the outer shell, not pressurized, are exposed to compressive forces from thrust and bending moments and only a small area in the upper tank region is supported by internal pressure. Relatively deep ellipsoidal bulkheads with an axis ratio of $\sqrt{2}:1$ to avoid compressive hoop stresses at the equatorial region and the long thrust cone are responsible for the excessive length of the unpressurized shell areas.



Now, the left half shows a much shorter vehicle of equal performance capability. The length reduction is caused by a multiple engine arrangement, common bulkheads and shallow ellipsoidal heads with an axis ratio of 2:1. Almost 70 percent of the outer shell is supported by internal pressure, against only 35 percent on the right. Internal pressure not only reduces compressive stresses in the shell from thrust and bending moments but also increases the buckling stress itself by as much as 70 percent.

With the shorter vehicle, bending moments due to lift and inertia forces are also reduced, approximately linearly with the length ratio.

There are certain penalties to pay for this ideal configuration. The engines require aerodynamic fairings exposed to aerodynamic heating. The common bulkheads require additional insulation and must be reinforced to withstand possible pressure differences causing an unfavorable buckling condition. Shallower bulkheads must be reinforced at the equator because any axis ratio greater than 2:1 leads to compressive hoop stresses in that region.

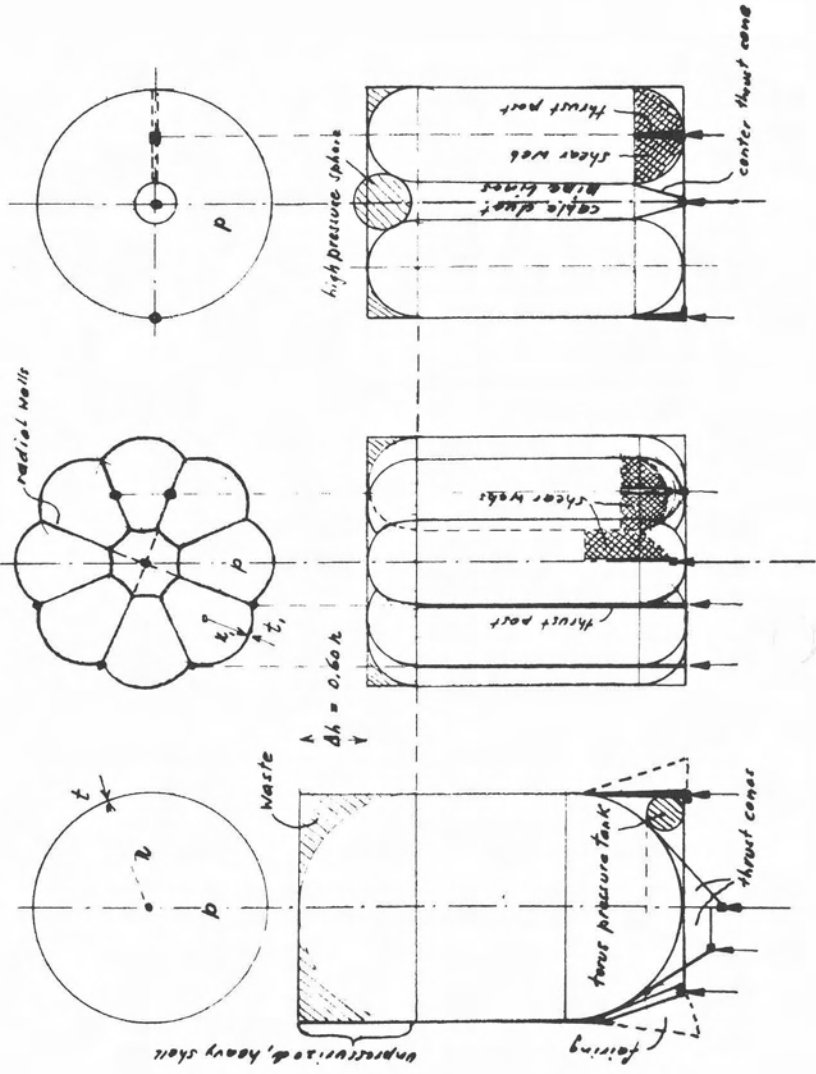
Monocoque propellant tanks should be designed so that the cylindrical wall thickness required for hoop tension due to internal pressure and the dynamic head pressure coincides with the wall thickness required to withstand axial compressive forces from thrust and bending moments. Propulsion requirements, however, might necessitate pressures different from "optimum" conditions. Low tank pressures, ribs and ringframes, integral to the tank wall, provide for a much more efficient design. High tank pressures reduce the structural design efficiency, but might improve propulsion system efficiency to obtain a net performance gain important for certain vehicle missions.

Different tank configurations are shown in Figure No. 2. On the left you see a conventional cylindrical tank. The multicell tank of equal volume, shown in the middle, reduces the vehicle length and waste space by providing shallow bulkheads. It also allows for thinner skin gages with higher weld efficiencies. Propellant sloshing frequencies are increased and effective sloshing masses are reduced. If engines can be arranged such that the thrust is led into longerons between cells, the weight of thrust distribution members is minimized. A single engine, attached to the center post, counteracts the inertia forces of the center portion of the liquid; however, additional stability against "falling through" of the center portion of the tank has to be provided by reinforcing portions of the radial walls to convert them into rigid shear webs. A multicell tank with radial walls is stable under internal pressure but unstable under hydrostatic or liquid inertia forces. This holds true also for a toroidal tank or a cylindrical tank with semitoroidal bulkheads shown on the right. Both tank configurations help reduce overall vehicle length and weights and reduce the length of unpressurized intertank shells.

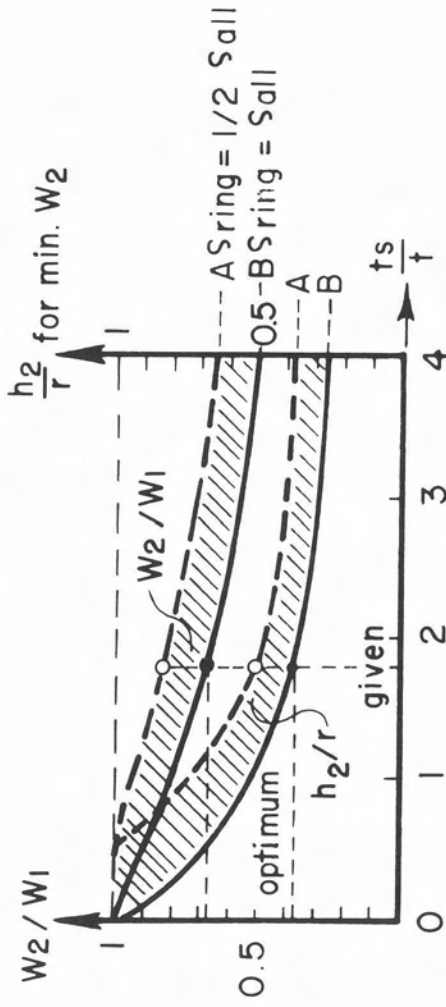
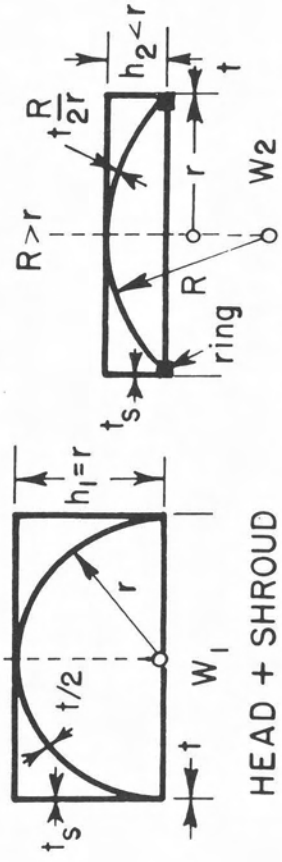
Figure No. 3 shows weight savings possible by using flat spherical segments and thrust rings instead of hemispherical bulkheads. Considerable saving is achieved by shortening of shrouds in areas of large compressive forces due to bending moment and thrust, where t_s , the distributed thickness of shroud walls, stringers, ringframes, and local reinforcements is greater than the tank wall thickness. Similar considerations hold for ellipsoidal bulkheads since the weight of those is close to the weight of a ring and spherical segment of the same depth.

$$A_s = 0.40 h$$

$$t_s = 0.40 t$$



BULKHEADS FOR MINIMUM WEIGHT



Time allows me to briefly touch on only one other important problem:

Dynamic Ground Testing of Complete Space Vehicles

Theoretical analysis or model testing of large, complex vehicle structures do not reveal the true dynamic behavior to the extent that is needed to properly adjust guidance computer gains or electronic filters to minimize elastic structural and control interference. In order to gain insight into local modes and complex dynamic responses such as engine-actuator-bending mode coupling with lateral vehicle modes, it is necessary to do full scale dynamic testing. Figure No. 4 shows a Saturn I vehicle suspended vertically on cables and springs in a 250 foot high tower to simulate in-flight bending, torsional, and longitudinal vibrations. At several stations along the vehicle, platforms provide access and shaker force inputs. We cannot have the vehicle suspended horizontally because under a 1G load lateral bending stresses of a full or partially filled vehicle exceed design stresses by a factor of 4 - 6. The highest in-flight lateral load due to side winds, gusts and maneuvers seldom exceeds 0.3G.

Snubbers at the top prevent excessive leaning over of the vehicle under high ground winds during testing. Figure No. 5 indicates the boundary restraints for proper simulation of free flight, that is free-free lateral bending mode conditions. For stable rigid body motion the restoring moment of the cable and spring suspension must be larger than the weight times the excentricity created by the rocking over. This means

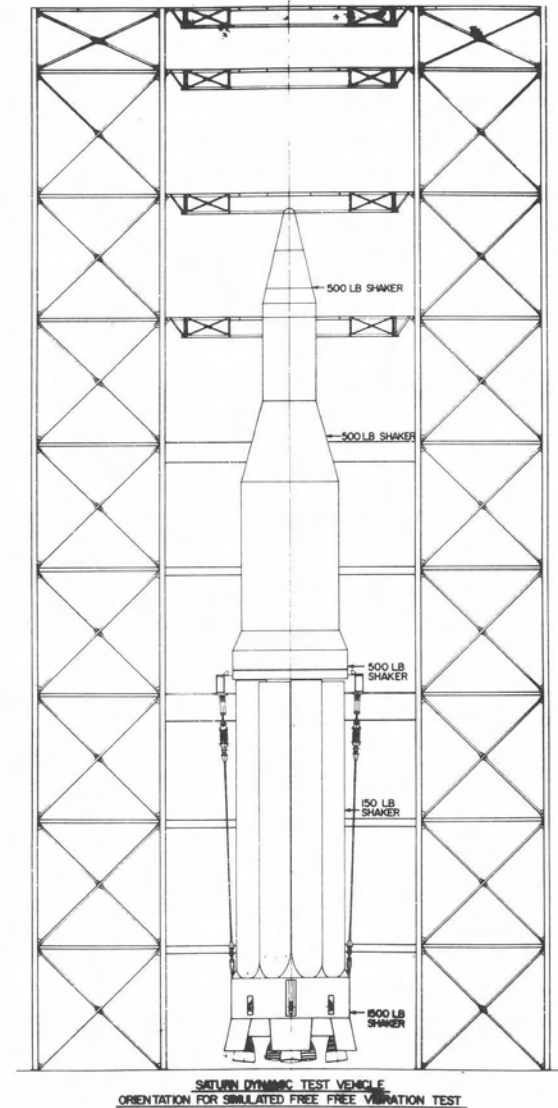
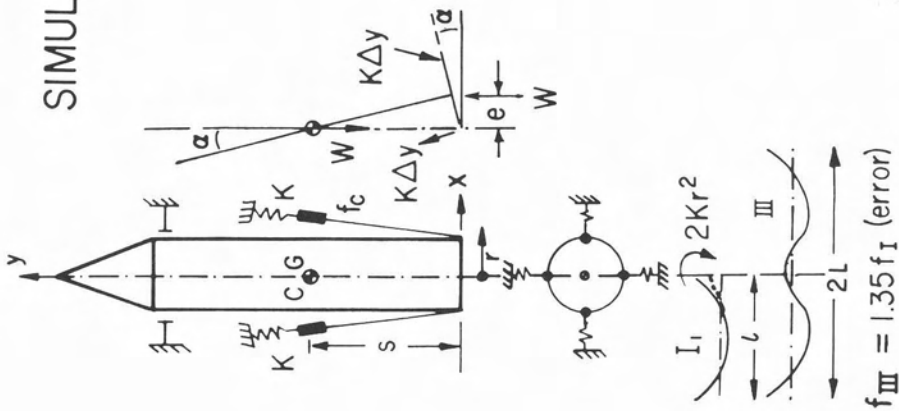


FIGURE 4

SIMULATION OF FLIGHT BENDING MODES



for stable motion

$$M_{\text{restg.}} > W_e$$

$$2Kr^2 > W_s$$

$$f_r = \frac{1}{2\pi} \sqrt{\frac{2Kr^2 W_s}{\theta}} < \frac{f_{1b}}{10}$$

$$2Kr^2 > 0.04\pi^2 f_{1b}^2 \theta + W_s$$

$$450,000 \text{ lb/ft} > K > 250,000 \text{ lb/ft}$$

$$f_x = \frac{1}{2\pi} \sqrt{\frac{g}{s}} = 0.13 \text{ cps}$$

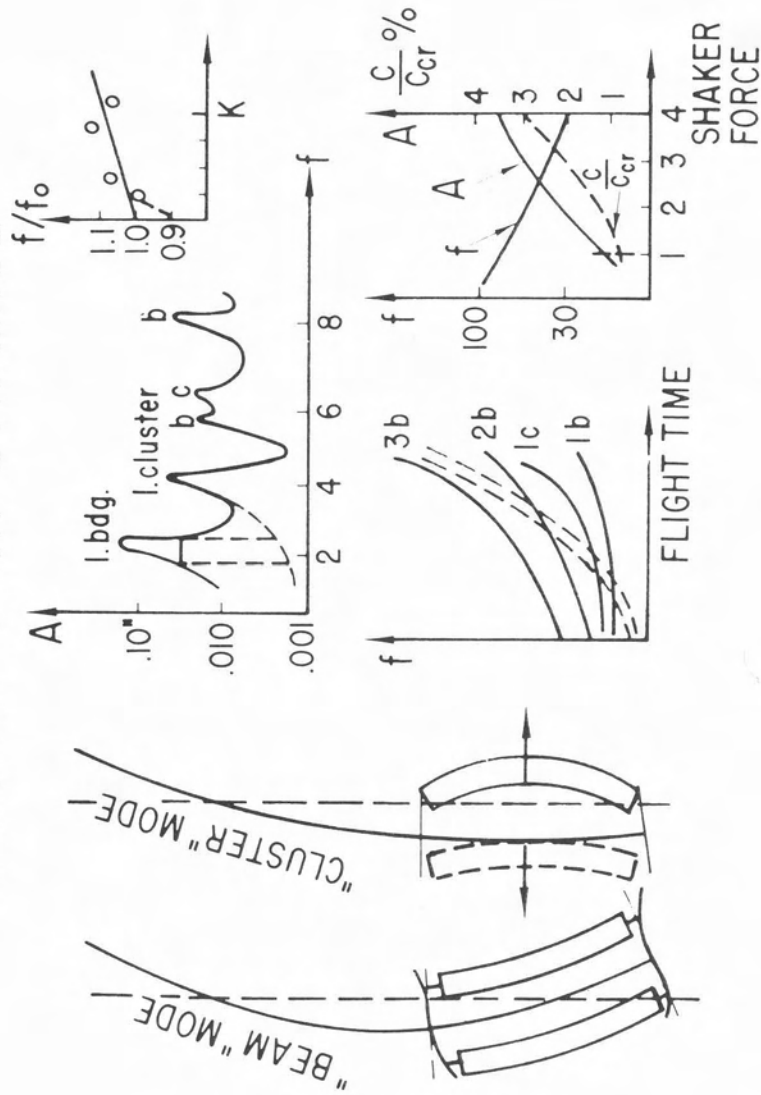
$$f_y = \frac{1}{2\pi} \sqrt{\frac{4Kg}{W}} = 1.21 \text{ cps}$$

$$f_c = \frac{1}{2} \sqrt{\frac{sg}{pe^2}} = 4 \text{ cps !}$$

that $2Kr^2$ must be larger than W_s . The other limitation is that the springs should be soft enough so that the rigid body rocking frequency is not more than about 10 percent or 20 percent of the first bending frequency. This gives a second equation for the maximum K allowable for a given vehicle. In case of Saturn, we find that the spring constant should be larger than 250,000 pounds per foot in order to have stable motion, but it also should be smaller than 450,000 pounds per foot to keep the rocking frequency low. With this suspension configuration we find that the translatory frequency is 0.13 cycles per second, the vertical frequency is 1.21 cycles per second and the rocking frequency in this case is about 0.30 cycles per second. Now the first bending in the Saturn I is about two cycles per second so we can see that the rigid body suspension frequencies are sufficiently below the bending modes so as not to couple with them. However, we found that our suspension cable frequency crossed through and coupled strongly with several bending modes and we had to install clamps for tuning the cables towards higher frequencies to eliminate response interference.

Figure No. 6 deals with the complex dynamics of the clustered Saturn I vehicle. It shows the basic beam bending frequencies and cluster frequencies versus flight time going up as you lose mass from the booster and in between two other curves which are the frequencies of outer lox and fuel tanks responding as simple beams between upper and lower tie-in points. Outer tank individual frequencies cross through all of the main vehicle "beam" frequencies during flight. Whenever this is the case, it is

CLUSTER TANK DYNAMICS



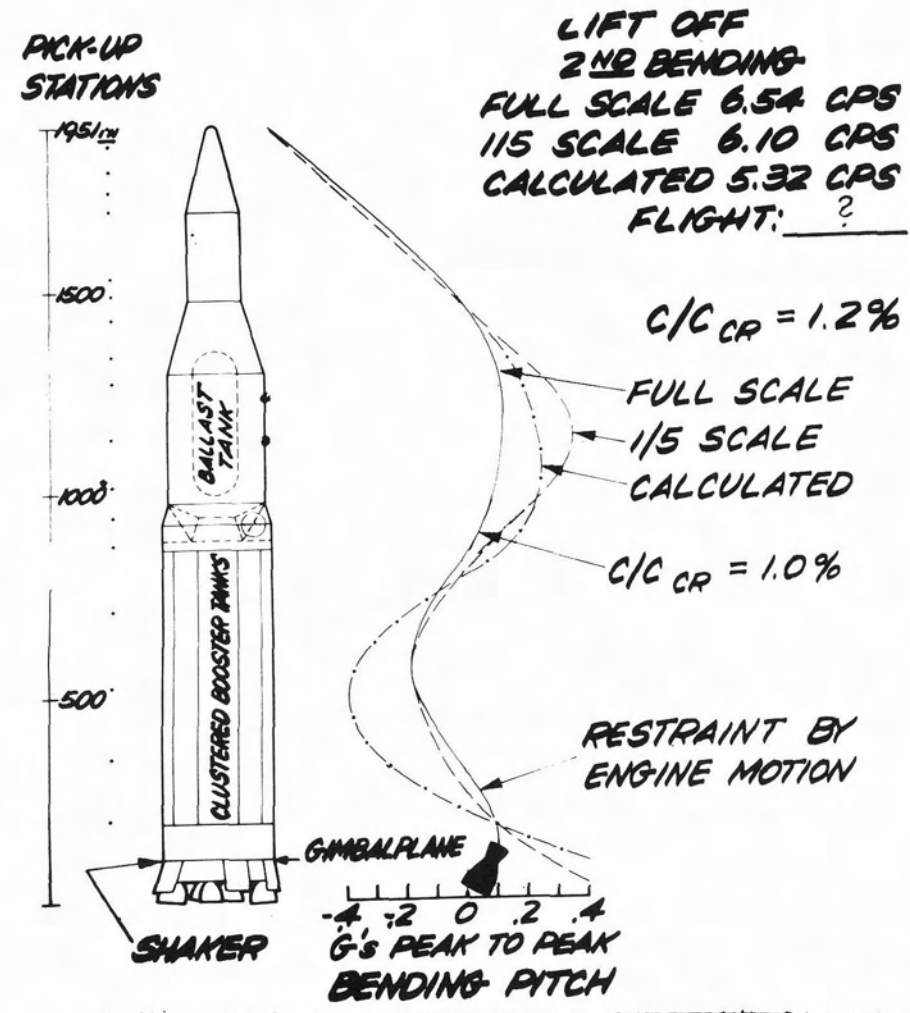
difficult to really identify the modes. Furthermore, we did not know exactly how strong our restraining moment was in our suspension, so we varied the spring constants to a certain degree and tried to establish a trend as indicated on the upper right hand corner.

Experimenting with different numbers of cables and springs per cable (4, 8, and 12) we obtained 4 check points, unfortunately with some dispersion and were able to draw a trend line and extrapolate it through the ideal case $K=0$. The dispersion is partially due to local compliance of the tail structure of the vehicle. This produced a spring in series effect overshadowing the changes in cable spring stiffnesses. Our suspension system raised all frequencies by 5 percent to 10 percent, which is tolerable frequency wise, but it changed the mode shapes too and in such a way that local responses and especially local slopes were distorted. Therefore, transfer functions - for instance rate gyro outputs over lateral force inputs at the engine gimbal points, so important for guidance computer settings, cannot be reproduced with accuracy. Force measurements with strain gages on the suspension links helped to correct the input values and to approach free flight transfer function characteristics. A great concern to us was coupling of vehicle and suspension damping, because the damping of springs and cables was considerably higher than the vehicle damping and would have lead us to assume too high damping values for the vehicle. Detuning of cable frequencies helped to separate these influences, together with a reduction of suspension system mass and increase of cable

tension. We also found that the "vehicle plus suspension" system was not linear. The amplitude lagged the increase of shaker force, the frequency dropped slightly and damping increased as indicated in the lower right hand corner of Figure No. 6. In spite of these difficulties, full scale dynamic ground testing of the Saturn increased our knowledge of this vehicle's dynamic behavior more than even the most refined analysis could have done. On the other hand, full scale testing gave us many ideas for analytical improvement. In the near future, we should be able to confine our testing to on-pad cantilever conditions, correlate test results with analysis and then extrapolate analytically to predict in-flight dynamic behavior of future vehicles.

Figure No. 7 shows a comparison of a calculated mode with test results from full scale and 1/5 scale tests. The differences are mainly due to inadequate scaling of engine and actuator elastic tie-ins and the simplifying analytical assumption that the engines are a simple extension of the beam that represents the vehicle. In reality the engines and actuators behaved like tuned dampers and restrained second bending modes considerably. Figure No. 8 compares model, prototype, analytical and flight results on the basis of average values and points out the merits of full scale testing, especially as far as mode representation goes. The 1/5 scale model and theoretical mode calculations deviate as much as 40 percent from flight modes especially with higher modes and frequencies. However, the scale model alerted us long before we started prototype testing that the engines would

MODE COMPARISON



FOUR-WAY COMPARIISON OF MODEL, PROTOTYPE, ANALYSIS, AND FLIGHT RESULTS

	<i>FLIGHT</i>	<i>PROTOTYPE</i>	<i>MODEL</i>	<i>ANALYSIS</i>
<i>FREQUENCY</i>	<i>100</i>	<i>100 ± 5</i>	<i>100 ± 5</i>	<i>100 ± 15</i>
<i>MODE SHAPE</i>	<i>100</i>	<i>100 ± 15</i>	<i>100 ± 40</i>	<i>100 ± 40</i>
<i>DAMPING</i>	<i>—</i>	<i>100</i>	<i>100 ± 10</i>	<i>—</i>

couple with second bending modes. It also gave us good indications of the damping to be expected and proved that a vertical suspension system was feasible and practical. The model was also useful in certain parametrical studies where we tried to suppress outer tank motions. We tried using bands and blocks to tie all nine tanks together, but model testing convinced us that only continuous and rather heavy shear ties would weld the tank cluster into a single unit. Similar modifications of the prototype would have been expensive and time consuming. In order to further improve our dynamic model techniques, we are fabricating a 1/10 scale model of the Saturn V, the "moonrocket," and will start testing it soon to weed out dynamic bugs, if any, and be prepared for the great day when the first vehicle leaves the launching pad at Cape Kennedy.